Enhanced Water Recovery in the Coal Seam Gas Industry using a Dual Reverse Osmosis System

Dean Blair, Dominic T. Alexander, Sara J. Couperthwaite, Mariam Darestani and Graeme J. Millar*

Institute for Future Environments and School of Chemistry, Physics & Mechanical Engineering, Science and Engineering Faculty, Queensland University of Technology (QUT), Brisbane, Queensland 4000, Australia

Mining of brines produced in the coal seam gas industry for water and salts is of major concern globally. This study focussed on the use of a dual stage reverse osmosis system to achieve high water recovery rates. It was our hypothesis that an intermediate nanofiltration stage was required to stabilize the performance of the second reverse osmosis stage. The second stage RO membrane was found to be fouled by silica and aluminosilicates when used with any intermediate brine treatment. Theoretical predictions using PHREEQC software supported the experimental outcomes in terms of identifying species with high scaling potential. Coagulation of the coal seam brine using aluminium chlorohydrate was found to remove up to 70.5 % of dissolved silica and thus this method may be useful for prevention of fouling of downstream membranes. ROSA software was also employed to enable selection of possible nanofiltration membranes to treat the coal seam brine sample. Tighter membranes were found to exhibit significantly higher rejection of ions responsible for scale formation during brine concentration operations. Albeit, the flux rates were less than the looser membrane types. A pressure of 20 bar was suggested to be practical for the nanofiltration stage as the flux rate more than doubled from the flux estimated at 15 bar. An intermediate nanofiltration stage perhaps combined with a coagulation step is recommended for use in a dual stage RO system to concentrate coal seam brines.

Keywords: coal seam gas; coal bed methane; reverse osmosis; brine; modelling; scaling; membrane

* Corresponding Author

Prof. Graeme J. Millar;

Science and Engineering Faculty | Queensland University of Technology

P Block Level 7, Room 706, Gardens Point Campus

ph 07 3138 2377 | mobile 0425 815 148 |email graeme.millar@qut.edu.au

1. Introduction

Development of unconventional gas resources, such as coal seam gas (CSG), has expanded in recent years [1-3]. Australia possesses large deposits of CSG, with an estimated resource of 4.3 trillion m^3, and is currently the world's second largest CSG producer, behind the USA [3]. Current annual production of CSG in Australia is 6.2 billion m^3 and this is expected to grow until 2030 to meet increasing global demand [1]. CSG is comprised mainly of methane, which is present alongside water in fractures within coal seams [4]. Due to the poor solubility of methane, the majority of the gas is adsorbed onto the coal surfaces, where it is trapped in place by water pressure [4]. In order to extract the gas, the coal seam must be depressurised by pumping out the water, which allows the gas to desorb, coalesce into bubbles and rise to the surface with the water [4]. Consequently, CSG extraction is accompanied by the production of large volumes of water as a by-product. By 2030, an estimated 300 GL of CSG water will be produced each year in Australia [4]. Management of this water for beneficial reuse options is therefore a key issue in the CSG industry [5]. Proposed uses for CSG water include coal washing, dust suppression, irrigation, livestock watering, aquaculture, industrial and manufacturing use, regeneration of depleted aquifers and purification for drinking water [1]. However, the potential environmental impacts of the water, resulting mainly from its high salinity, normally make it unsuitable for disposal or reuse without prior treatment [6]. The ideal goal of CSG water treatment is to recover the maximum amount of water and reuse the salt content [1].

The composition of CSG co-produced water can vary greatly from one site to another depending upon geological factors such as the depth of the coal seam, the composition of the surrounding rock, the length of time the water is exposed to the rock, and the origin of the water entering the coal seam [6]. CSG water is typically characterised by total dissolved solids (TDS) concentrations in the brackish range of 200-10,000 mg/L, although TDS levels of up to 39,260 mg/L have been reported in the USA, as well as alkaline pH values between 7.5 and 9 [1]. The primary dissolved species in CSG water are sodium, chloride and bicarbonate, which on average account for greater than 95% of the total ions in the water [3]. In the USA, CSG water is typically dominated by dissolved sodium bicarbonate; while in Australia the presence of sodium chloride type water is more common. Other species typically present in lower concentrations include potassium, calcium, magnesium, strontium, barium,

iron, aluminium and sulphate [1]. Silica is another species commonly found in CSG water, which can be present in the form of dissolved or colloidal silica [1]. Additional trace elements may also be present such as other metals, metalloids and boron [1]. Since CSG water has been in contact with coal, the presence of a wide range of organic species in the water is also common, including organic acids, polycyclic aromatic hydrocarbons, phenols and aromatic amines [1, 4].

Ion exchange (IX) [7] and reverse osmosis (RO) [8] are the desalination techniques most commonly employed by the CSG industry to treat co-produced water, with RO being the most widely employed in Australia to date [6]. Ultimately, a preferred goal is recovery of salts from the water in the form of valuable commodities. For example, Simon *et al*. [9] applied membrane electrolysis (ME) to coal seam brine in order to recover sodium hydroxide. It was noted that energy and desalination efficiencies depended upon the brine salinity, with higher brine concentrations requiring relatively less energy consumption but the degree of desalination concomitantly decreased. The degree of sodium bicarbonate species present in solution compared to sodium chloride also impacted the concentration of sodium hydroxide which could be produced. Duong *et al.* [10] more recently investigated the combination of membrane distillation (MD) and membrane electrolysis to recover purified water and sodium hydroxide from reverse osmosis brine derived from treatment of CSG water. Overall, the energy savings recorded by coupling of the MD and ME systems was significant.

For efficient water treatment, it is advantageous to maximise the amount of water recovered in the permeate stream and consequently minimise the amount of waste brine. One way in which this can be achieved is by employing a two-stage RO treatment process, in which additional permeate is recovered by treating the brine from the initial RO stage in a secondary RO stage [1, 11]. As a result of the elevated concentrations in the brine, this secondary RO stage is more susceptible to membrane fouling and scaling [11]. Membrane scaling refers to the precipitation of inorganic species onto a membrane surface, which occurs when the solubility limits of these species are exceeded as they accumulate in the retentate stream [12]. Common species responsible for scale formation during RO treatment of CSG water are carbonate and sulphate salts of divalent ions, such as calcium,

magnesium, strontium and barium, as well as silica and metal silicates, particularly aluminium silicates [13, 14]. Scale formation leads to reduced membrane performance and necessitates periodic cleaning of the membrane surface, which reduces membrane life and increases operating costs [1]. Membrane scaling is therefore recognised as one of the major limitations encountered in high recovery RO operations, including two-stage RO treatment of CSG water [14]. The Wild Turkey plant operated by Petro-Canada at the Powder River Basin in the USA employed media filtration, chlorine addition and acid dosing followed by two-stage RO to treat 20 ML of CSG water per day at an overall recovery of greater than 90% [15]. The subsequently opened Mitchell Draw facility, capable of treating 12 ML of water per day, added ion exchange softening prior to the RO stage [15]. This latter step reduced the potential for scale formation by removing scale forming ions such as calcium and magnesium, which reduced the need for acid dosing and consequently allowed the system to operate at a higher pH. This in turn increased the solubility of silica and dissolved organic species, reducing silica and organic based fouling, and shifted the boron equilibrium from boric acid to borate, leading to improved boron rejection [15].

A spiral wound RO configuration is most commonly used, as this configuration offers the advantages of high specific membrane surface area, easy scale-up, interchangeability and low production and replacement costs [16]. Spiral wound RO configurations can achieve a maximum operating pressure of approximately 70 bar [17]. For highly concentrated feed systems, disc tube RO (DTRO) is an alternate configuration which enables RO operation at higher pressures than is possible with spiral wound systems [17]. The disc tube module consists of two RO membranes sealed together with a permeate spacer between them. Stacks of these membrane elements, separated by feed spacers, are placed within a pressure vessel. The feed water flows tangentially across one side of a membrane element, then back across the other and water that passes through the membrane is carried through the permeate spacer to a central permeate collection tube [18]. The disc tube module design allows RO operation at pressures of up to 200-300 bar and has been widely employed in the treatment of highly concentrated landfill leachates [17, 19].

Nanofiltration (NF) is a membrane separation technique similar to RO, where NF membranes are characterised by larger pore sizes, which leads to the selective removal of

multivalent ions, such as calcium and magnesium, over monovalent ions while allowing for lower operating pressures [20]. Consequently, NF has been successfully implemented in water softening applications and as a pre-treatment step to prevent hardness based scale formation during RO desalination [20, 21]. In one such case, an intermediate NF step was incorporated in a two-stage RO treatment of dumpsite leachate to remove divalent scaling species from the first stage brine, leaving a permeate containing primarily monovalent species which could be treated by secondary RO without the risk of scale formation [22]. In this latter example the NF module enabled the treatment process to operate at an overall permeate recovery rate of 95 % [22].

It is our hypothesis that the combination of a nanofiltration unit as an intermediate stage in a dual reverse osmosis system wherein the second RO unit is a disc tube RO configuration may allow mining of reverse osmosis brine solutions for maximum water recovery. Concentration of the remaining dissolved salts may also promote the economics of salt recovery. The overall aim of this project was to assess the viability of an intermediate NF step as a method of scale prevention during secondary RO treatment of CSG brine. As such, the following research questions were addressed: (1) What is the typical composition of CSG brine produced from an operating CSG facility; (2) Can modelling software be employed to predict the species likely to be responsible for scale formation on RO membranes and equipment; (3) Which species foul membranes in a dual RO process for CSG water treatment; (4) Do theoretical predictions correlate with deposits identified on RO membranes; (5) Which membranes are recommended (6) What is the impact of use of a nanofiltration stage upon CSG brine composition. To answer the latter questions we obtained CSG brine produced in an RO plant in the Surat Basin, Queensland. PHREEQC software was used to estimate which inorganic species may exhibit significant scaling potential and scale deposits on a used membrane from a DTRO secondary desalination unit were characterized by a combination of Scanning Electron Microscopy (SEM) and infrared spectroscopy (FTIR). ROSA software was used to aid in membrane selection and a laboratory scale nanofiltration membrane was tested for ability to reject scale forming species from solution.

2. Materials and Methods

2.1 Water Analysis

Brine resulting from reverse osmosis treatment of CSG water was supplied by an operating CSG company in the Surat Basin, Queensland. The pH, conductivity and reduction potential of the CSG brine were measured using calibrated handheld probes (TPS-Aqua). Notably, these latter methods were employed to test brine which had been transported and stored for a period of time (less than 2 weeks). As such, it should be noted that these values may differ from those which may have been obtained from direct measurements on the RO plant. Due to health and safety aspects and logistical issues associated with the remoteness of the CSG operation it was not possible to sample otherwise. Five undiluted brine samples, as well as five samples diluted by a factor of 1:10 with 2.5% HNO_3 using an autodiluter (Hamilton MicroLAB 600), and five samples diluted by a factor of 1:100, were prepared and analysed with ICP-OES (Perkin Elmer Optima 8300) to determine the concentrations of key elements. The chloride concentration was determined using potentiometric titration with 0.1N $AgNO_3$ solution, performed in triplicate using a Mettler Toledo T50 auto-titrator. Alkalinity was determined by manual titration with a 0.1N HCl solution, which was standardised against a prepared Na_2CO_3 solution *via* titration with methyl red. The alkalinity titration was performed in triplicate with fixed endpoint pH values of 8.3 and 4.5, representing the carbonate and total alkalinity respectively, with the difference representing bicarbonate alkalinity. Lastly, three samples of CSG brine diluted by a factor of 1:40 with ultrapure water, filtered using a 0.45 micron syringe filter and analysed with a GE Sievers InnovOx laboratory TOC analyser to determine the non-purgeable organic carbon (NPOC) content of the water.

2.2 Membrane Autopsy

Fresh and used RO membranes from a second stage RO unit which was used to concentrate CSG brine were obtained the operating company. The identity of the used RO membrane is not reported due to considerations of commercial confidentiality. A Leica M125 stereo optical microscope was used to observe and image the surface of the clean and used membranes at up to 10x magnification. Representative samples of the used membrane were then cut and mounted on aluminium sample studs with double-sided carbon tape. The samples were sputter coated with gold (Leica EM SCD005, thickness 10 nm), then the

surface layer was imaged, with accompanying EDS spectra, using a JEOL JSM-7001F field emission scanning electron microscope (accelerating voltage 20 kV, working distance 10 mm). Additional samples of the used membrane were cut and mounted vertically in Epofix resin blocks to obtain cross-sections of any scale deposits found. The surfaces of these blocks were polished successively with 1200 grit SiC paper, a 9 µm diamond polish, a 3 µm diamond polish and a 1 µm diamond polish, then sputter coated with gold. SEM images and accompanying EDS spectra of the cross-sections were then obtained. Membrane samples were also cut and mounted on sample studs, then imaged with a Hitachi TM3000 desktop SEM (accelerating voltage 15 kV, working distance 12 mm) to obtain elemental mapping of the membrane surface for the elements C, O, S, Na, K, Cl, Ca, Mg, Fe, Al and Si. A Thermo Scientific Nicolet iS50 diamond ATR-FTIR instrument (64 scans, resolution 4 cm^{-1}) was used to obtain absorbance IR spectra (500-4000 cm^{-1}) of the surfaces of clean and used membrane samples. A spectral subtraction was then performed to identify the peaks in the used membrane spectrum to determine the presence of species which were not part of the original membrane composition.

2.3 Coagulant Test

Silica removal using coagulant addition was investigated using Alchlor Gold (Hardman Chemicals), a commercial aluminium chlorohydrate based coagulant. A Platypus Jar Tester was employed which allowed for the parallel testing of 4 water samples. While stirring vigorously, 50, 100, 250, 500 and 1000 µL volumes of Alchlor Gold were added to separate beakers containing 500 mL of CSG brine, which were then stirred gently for one hour. At the end of this time, the resulting suspensions were allowed to settle for 20 minutes, then a 10 mL volume of each solution was collected and filtered through a 0.45 µm syringe filter. From these volumes, three samples diluted by a factor of 1:10 with 2.5% HNO_3 were prepared and analysed using ICP-OES. The degree of silica removal was calculated using the concentration determined from ICP-OES before and after coagulant addition.

2.4 Modelling

The PHREEQC 3 software package was employed to predict the saturation indices of a range of mineral phases in the CSG brine at 25°C, using the measured composition data and the

phreeqc.dat database file [23]. The brine was then concentrated 4-fold within the software to simulate RO operation at 75% recovery and the saturation indices were recalculated.

The ROSA 9 software package from DOW was used to predict the performance of the NF pre-treatment step. ROSA software has been applied in several studies of desalination processes and is widely used in industry [23, 24]. The feedwater composition was specified using the measured CSG brine composition data, then NF performance was modelled at 25°C for a one-pass system containing a single NF90-2540 or NF270-2540 membrane element, with a feed flow rate of 0.30 m^3/h and feed pressures of 12.5, 15, 17.5, 20 and 22.5 bar.

2.5 NF Performance Test

NF membrane performance was evaluated with a Sterlitech HP4750 stirred membrane test cell. The HP4750 cell is a dead-end filtration unit that utilises 47 mm diameter membrane discs. Four NF membranes were tested, NF90 and NF270 (Dow Filmtec), TS80 (TriSep), and HL (GE Osmonics). The properties of these membranes are shown in Table 1.

Table 1: Description of nanofiltration membranes used in CSG brine treatment tests

Series	NF90	NF270	TS80	HL
Type	Low Energy/Low Pressure	Organics Removal, Softening	Softening	Softening
pH Range	2-11	2-11	2-11	3-9
Flux(GFD)/psi	46.0-60.0/130	72.0-98.0/130	20/110	39/100
NaCl Rejection			80-90%	
$MgSO_4$ Rejection	99.0%	99.2%	99.0%	98.0%
MWCO (Da)	~200-400	~200-400	~150	~150-300
Polymer	Polyamide	Polyamide	Polyamide	Thin Film

Prior to each test, the membranes were immersed in ultrapure water for 24 hours, then the cell was assembled and ultrapure water was filtered through the membranes at the desired operating pressure until a stable flux rate was observed. Once pre-conditioning of the membranes was complete, the cell was filled with approximately 250 mL of CSG brine, which was filtered at the desired operating pressure until 50 mL of permeate was collected. The time taken to do so was recorded and used to calculate the permeate flux rate. Separate tests were conducted at 15 and 20 bar for each membrane. In all tests, the feed solution was stirred at 300 rpm. Permeate was prepared and analysed with ICP-OES in the same way as the initial CSG brine. Rejection values for the important scaling species were calculated using the concentrations determined by ICP-OES in the original brine and permeate.

3. Results and Discussion

3.1 Water Composition

Table 2 shows the composition and physical properties of the brine sample investigated in this study. As expected from previous analysis of CSG water [6, 25], sodium, chloride, and bicarbonate ions were the most prevalent dissolved species. Calcium and magnesium, and to a lesser extent strontium and barium, were also present. Compared to the brackish groundwater RO brine outlined by Walker *et al.* [26] the levels of alkaline earth ions in the brine were substantially lower (*e.g.* 16.2 and 13.3 mg/L Ca & Mg, respectively compared to 612 and 326 mg/L for the same elements from the USA sample). The solution pH of 8.6 was in the range expected for CSG water [6] and reflective of the high alkalinity present in the sample. Silicon was also present at a concentration which has been indicated to potentially lead to islands of silica based scale on reverse osmosis membranes [27]. Aluminium and iron, which have been reported to enhance silica precipitation, were also present in the brine albeit can significantly lower concentrations than the dissolved silica. However, Antony [12] recommended that concentrations of aluminium and iron should be kept below 0.05 mg/L in order to minimise the possibility of silicate precipitation and notably in this instance both the latter species were in excess of the latter stipulated limits. It was assumed that the identification of phosphorous in the CSG was due to the presence of HPO_4^{2-} ions in solution which was the most likely species present at the solution pH of 8.6. The presence of phosphate species in CSG water or brine has not often been reported [6, 28, 29]. One possibility for the concentration of phosphorous (phosphate) species in the CSG brine may be related to the application of phosphorus based anti-scalants to the feed water prior to first stage RO treatment [30]. A small amount of dissolved sulfur containing species was detected and according to known solution chemistry the major species at 8.6 should be SO_4^{2-}.

3.2 PHREEQC Modelling

Table 3 illustrates the data calculated from application of PHREEQC to the brine composition shown in Table 1. Scaling is a thermodynamic process involving a phase change, which requires a level of supersaturation [31]. The scaling potential of a given species can therefore be expressed using the saturation index (SI):

$$SI = \frac{IAP}{K_{sp}}$$

Where IAP and K_{sp} are the ion activity product and solubility product of that species, respectively [12]. A saturation index greater than unity indicates that a given species is supersaturated and that scaling may occur [12]. Factors influencing the scaling potential include ion concentration, pH, temperature, fluid velocity and operating pressure as well as the presence of other salts or metal ions [1, 12].

Table 2: Composition and physical properties of for the single CSG brine sample used in this study

pH	8.6
Reduction Potential (mV)	254.0
Total Dissolved Solids (mg/L)	15600
NPOC (mg/L)	43
Total Alkalinity (mg/L $CaCO_3$)	5730
Carbonate Alkalinity (mg/L $CaCO_3$)	540
Bicarbonate Alkalinity (mg/L $CaCO_3$)	5190
Chloride (mg/L)	5924.3
Na (mg/L)	6207.6
K (mg/L)	30.2
Ca (mg/L)	16.2
Mg (mg/L)	13.3
Hardness (mg/L $CaCO_3$)	95.35
Sr (mg/L)	6.9
Ba (mg/L)	4.37
Si (mg/L)	36.46
Al (mg/L)	0.49
Fe (mg/L)	0.074
Li (mg/L)	1.07
B (mg/L)	0.77
Cu (mg/L)	0.13

Mn (mg/L)	0.093
Rb (mg/L)	0.23
S (mg/L)	0.23
P (mg/L)	5.48

Table 3: Prediction of Supersaturation of Inorganic species in CSG Brine using PHREEQC

Name	**Formula**	**log(SI)**	**log(SI) at 75% Recovery**
Albite	$NaAlSi_3O_8$	2.78	6.07
Anorthite	$CaAl_2Si_2O_8$	-0.65	2.31
Aragonite	$CaCO_3$	1.22	1.80
Ca-Montmorillonite	$Ca_{0.165}Al_{2.33}Si_{3.67}O_{10}(OH)_2$	3.99	8.64
Calcite	$CaCO_3$	1.37	1.94
Chalcedony	SiO_2	0.34	1.05
Chlorite(14A)	$Mg_5Al_2Si_3O_{10}(OH)_8$	6.43	9.01
Chrysotile	$Mg_3Si_2O_5(OH)_4$	1.01	1.64
Dolomite	$CaMg(CO_3)_2$	3.07	4.22
$Fe(OH)_3$ (a)	$Fe(OH)_3$	1.63	2.35
Gibbsite	$Al(OH)_3$	1.08	1.95
Goethite	FeOOH	7.53	8.26
Hematite	Fe_2O_3	17.07	18.54
Hydroxyapatite	$Ca_5(PO_4)_3OH$	3.63	5.28
Illite	$K_{0.6}Mg_{0.25}Al_{2.3}Si_{3.5}O_{10}(OH)_2$	4.54	9.14
K-feldspar	$KAlSi_3O_8$	2.80	6.05
K-mica	$KAl_3Si_3O_{10}(OH)_2$	10.57	15.59
Kaolinite	$Al_2Si_2O_5(OH)_4$	4.52	7.71
Quartz	SiO_2	0.77	1.48
Rhodochrosite	$MnCO_3$	0.44	1.05
Sepiolite	$Mg_2Si_3O_{7.5}OH{:}3H_2O$	1.02	2.61
SiO_2 (a)	SiO_2	-0.50	0.22
Strontianite	$SrCO_3$	1.52	2.04

Talc	$Mg_3Si_4O_{10}(OH)_2$	5.40	7.47
Witherite	$BaCO_3$	0.43	1.01

Analysis was conducted not only for the CSG brine from the first stage RO stage but also for brine produced in a second stage RO unit assuming 75 % water recovery. Silica based scalants were particularly prevalent in terms of the number of potential inorganic phases which could precipitate, including silica and several aluminium and magnesium silicates. Hardness based scalants are also present, in the form of calcium, strontium and barium carbonate, as well as dolomite, which can be attributed to the high alkalinity. Interestingly, manganese carbonate, which is not a widely reported scalant of RO membranes, was also supersaturated. Conversely, the sulphate salts of these ions, which represent another common scalant type, were not supersaturated and were therefore not expected to contribute to scale formation. This latter deduction was in harmony with the relatively low concentration of sulphur containing species in the CSG brine [Table 2]. Hydroxyapatite, a calcium phosphate species, was also supersaturated, due to the aforementioned high phosphorus concentration in the brine. Phosphorus can be present in anti-scalant compositions, and it has been reported that these species can break down to produce orthophosphate, which is free to form calcium phosphate scale [12]. Lastly, a handful of iron and aluminium oxides and hydroxides were also supersaturated, given the low solubilities of these species and the relatively high concentrations of iron and aluminium.

The purpose of conducting a second simulation at four times the initial brine concentration was to determine if any new scalant types became supersaturated as the concentration of the retentate stream increased during RO operation. Amorphous silica and anorthite, an aluminium silicate species, became supersaturated, however, no new types of scalant were introduced. It is noted that addition of suitable anti-scalants may provide one strategy to alleviate the predicted high propensity for material precipitation [32, 33].

The influence of concentration polarisation (CP) upon scaling potential should also be considered. CP refers to the accumulation of rejected species in a thin layer of water at the membrane surface, leading to a higher concentration at the surface than in the bulk solution. Thus, salts may become supersaturated at the membrane surface even though the

bulk concentration is below the saturation limit [12]. The extent of concentration polarisation is influenced by permeate flux and water recovery as well as the feed composition and temperature, membrane properties and RO configuration [12]. Additionally, where a bio-film or cake layer has formed on a membrane surface, this layer can hinder back diffusion of rejected ions, increasing the degree of concentration polarisation [1, 34]. CP is typically countered through cross-flow operation, as the fluid motion across the membrane surface disperses the accumulated ions, however, this technique becomes less effective when operating at higher recoveries [12, 35]. The mechanism of scale formation can be strongly influenced by the extent of concentration polarisation. At low cross-flow velocities, which correspond to a high degree of concentration polarisation at the membrane surface, surface crystallisation is the preferred scale formation mechanism, while at higher cross-flow velocities, where the degree of concentration polarisation is reduced, bulk crystallisation is favoured [12].

3.3 Membrane Autopsy

3.3.1 Optical Microscopy of Membrane from Second RO Stage

Optical microscopy revealed that the used membrane surface was decorated with brown deposits which showed evidence of a darker particulate matter scattered throughout this material.

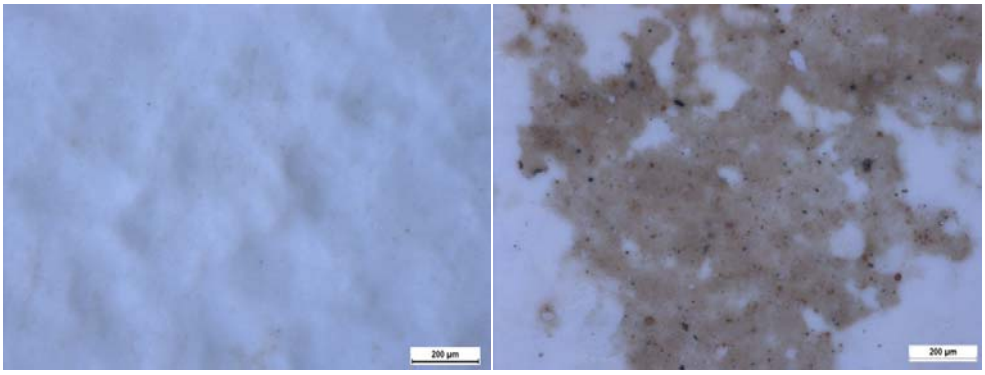

Figure 1: Optical microscopy images of clean membrane surface (left) and deposit on membrane surface (right) for a used secondary stage RO membrane which treated RO brine

Melián-Martel *et al.* [36] observed similar optical microscopy images when they examined an RO membrane which had been desalinating seawater. Patches of an orange-brown precipitate were noted on the used membrane especially in the vicinity of valleys of rough

membranes which were said to be caused by the presence of the spacers. The optical image of the used membrane also showed the presence of much smaller darker spots distributed over the main scalant surface similar to this study. Uchymiak *et al.* [37] applied an on line optical microscopy unit to detect the growth of scale deposits on a membrane surface and the growth of islands of scale on the membrane surface was observed to correlate with a decrease in membrane flux. In summary, it was evident that the membrane surface following desalination of brine from an RO unit treating CSG water, was decorated with contaminant species. At least two different types of foulant were detected, the identify of which is further investigated below.

3.3.2 Scanning Electron Microscopy (SEM) and Energy Dispersive Spectroscopy (EDS) Analysis of Membrane from Second RO Stage

Figure 2 shows both SEM images and EDS analysis of various sites on the used membrane sample from a secondary stage RO unit treating CSG brine. From the SEM images the scale layer appears to be predominantly formed of both micro-structured and amorphous phases. In terms of the micro-structured phase it was primarily comprised of silicon, sulphur, aluminium and sodium species, thus the presence of a sodium aluminosilicate and silica could explain the EDS analytical data. From PHREEQC calculations albite ($NaAlSi_3O_8$) was a primary candidate for the aluminosilicate identity. In some instances, larger crystalline deposits were noted and analysis suggested that these were composed of calcium sulphate species which was not in accord with the PHREEQC predictions which indicated that this species was under-saturated [Table 3]. Detection of carbon and sulphur was likely due to the EDS detecting the membrane beneath the scale layer, albeit the presence of carbonate and sulphate species could not unequivocally be dismissed. Other elements detected in minor quantities were calcium, magnesium, iron, potassium, and chlorine. Conversely, barium, strontium, manganese, and phosphorus were not detected, suggesting that materials comprising of the latter species did not form scale during the secondary RO treatment stage.

The results from this analysis were compared to a study conducted to identify the key potential scalants in RO brine from a CSG water treatment facility in Queensland. Zaman *et al.* [38] found that metal carbonate salts, particularly calcium and strontium carbonate,

were likely precipitates, while silica was also identified as a potential scalant. In supersaturated solutions, silica precipitation is proposed to occur through the polymerisation of monomeric silica to form silica colloids, which subsequently deposit on the membrane surface to form a cake layer [14]. However, silica can also react with metal ions to form metal silicates, most commonly aluminium silicates, which are less soluble than ordinary silica [14].

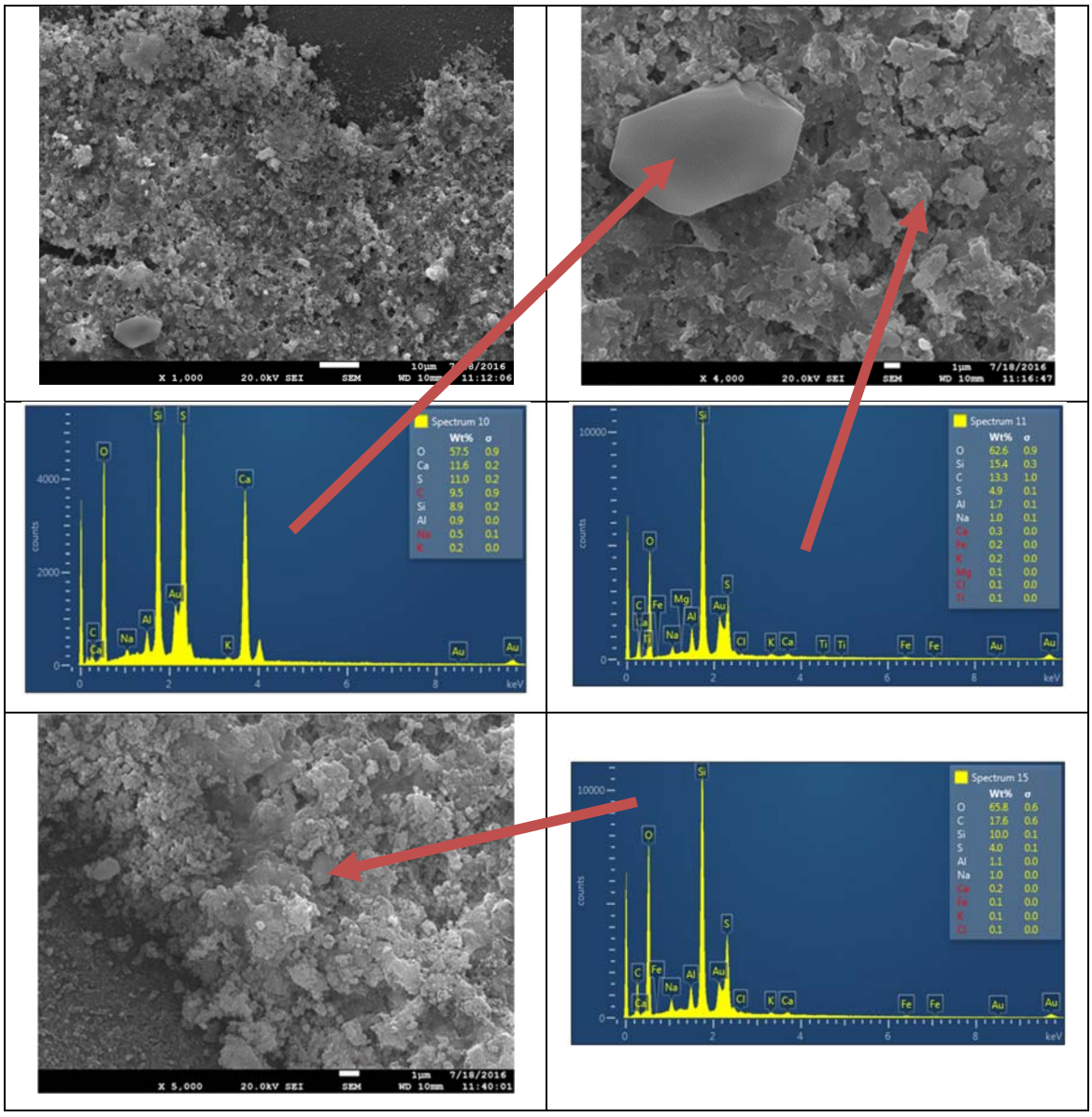

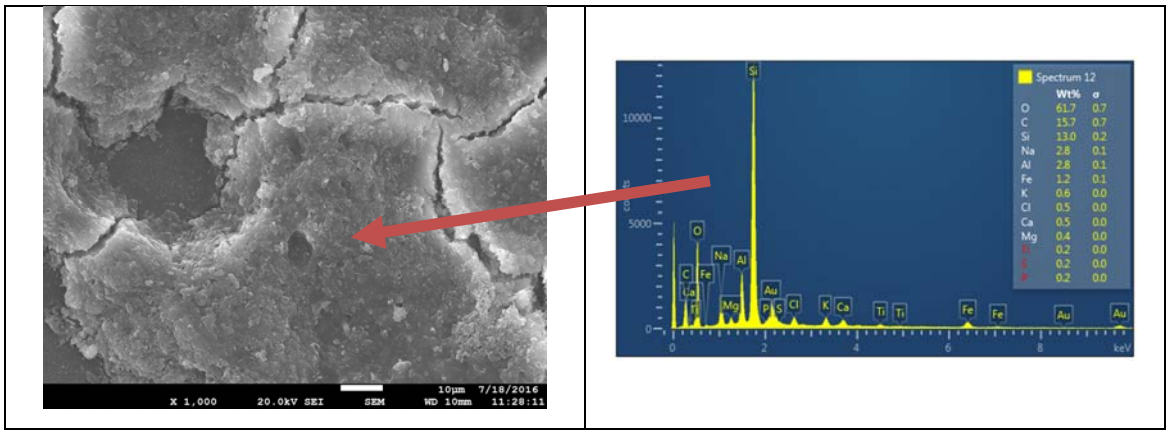

Figure 2: SEM images and EDS analysis of deposits on membrane surface for a used secondary stage RO membrane which treated RO brine

XRD revealed in the study of Zaman *et al.* [38] that a range of aluminosilicates formed including grandidierite and florkeite in addition to omongwaite, aragonite and hibbingite phases. These authors suggested that that silica could co-precipitate alongside metal carbonate salts [38]. While the formation and control of ionic scaling species is relatively well understood, the complex chemistry of silica precipitation has meant that silica-based scaling remains a major challenge in high recovery RO operations [39], and our study has confirmed this latter assumption. At the Wild Turkey facility in the USA, for example, silica scaling was identified as the primary factor responsible for limiting system recovery [15]. Additionally, in an RO pilot-scale study of CSG water treatment, Subramani *et al.* identified silica and aluminium silicate scaling as a key factor limiting system performance [40], again in agreement with this study.

Cross sections of the scaled membrane were also examined by SEM and EDS in order to determine the thickness of the deposits and to confirm if they were uniform in character.

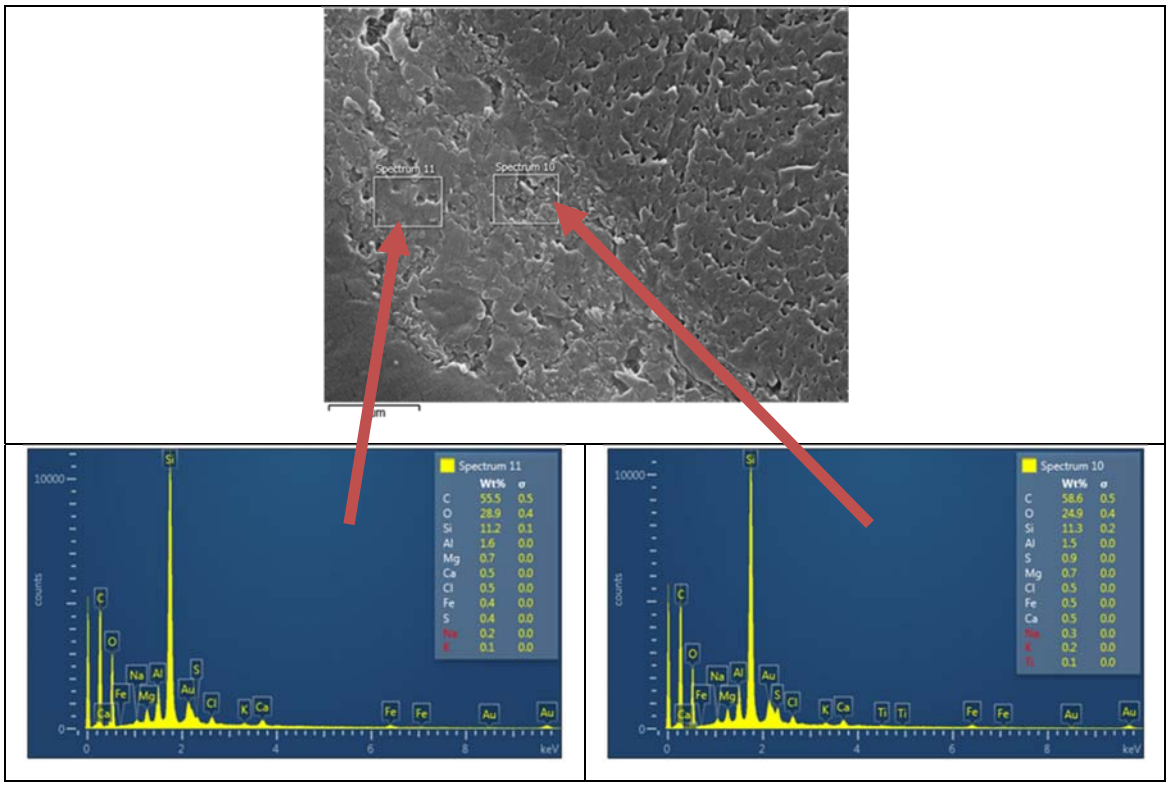

Figure 3: SEM and EDS analysis of a cross section of scale on used RO membrane

The SEM images of the scale layer cross-sections revealed that the thickness of the scale layer was up to approximately 5 µm and that its composition appeared uniform throughout. This was confirmed by the similarity of the EDS spectra taken at different points within the scale layer [Figure 3]. These spectra were also similar to those taken for the surface of the scale layer, with the exception that the proportion of carbon was much greater due to the presence of the resin used to mount the cross-sections.

3.3.3 Elemental Mapping of Scale Deposits on Used RO Membrane

Further information regarding the nature and distribution of the scale forming species on the RO membrane surface were elucidated by application of elemental mapping using the EDS function of the SEM instrument. Figure 4 revealed a strong positive correlation between silicon, oxygen, sodium, and aluminium, suggesting that aluminium silicates were a principle scaling species. This latter deduction was based upon the fact that aluminosilicates such as clays are commonly comprised of Na, Si, Al and O [41], and that aluminosilicate

deposits have been reported in studies of membranes employed for desalination [42, 43]. From the PHREEQC analysis [Table 3] albite was suggested to be a prospective mineral phase which was expected to be supersaturated in CSG brine. Recent work by Lunevich *et al.* [44] involved the application of ^{29}Si NMR to comprehensively investigate the formation of silica scale from solutions comprising of combinations of silica, sodium and aluminium species. When aluminium was co-present with dissolved sodium silicate, the rapid formation of possibly an aluminosilicate phase was postulated based upon disappearance of peaks ascribed to monomeric and dimeric silicates in solution. The presence of aluminium species appeared to promote the breakage of silicate bonds. Furthermore, in an investigation of CSG water treatment using RO, Subramani *et al.* determined from SEM-EDS and IR spectroscopy analysis that silica and aluminium silicates were the major scalant species [40]. Consequently, the elemental mapping data from this study supports the hypothesis that aluminosilicates can form on membrane surfaces during brine concentration.

Carbon and sulphur appeared as part of the membrane, but did not appear in the scale layer itself. Potassium, magnesium, and chlorine were relatively uniformly distributed across the membrane and scale layer, suggesting that their presence in the scale layer was not deemed important. The same is true for calcium and iron, however, these elements also manifested sporadically as small intense spots, corresponding with smaller deposits on the surface of the main scale layer. Based on the predicted scalant species [Table 3] and given the correlation observed between iron and oxygen, iron is most likely present as an iron oxide or hydroxide. In the case of calcium, there is insufficient evidence to determine in what form it is present.

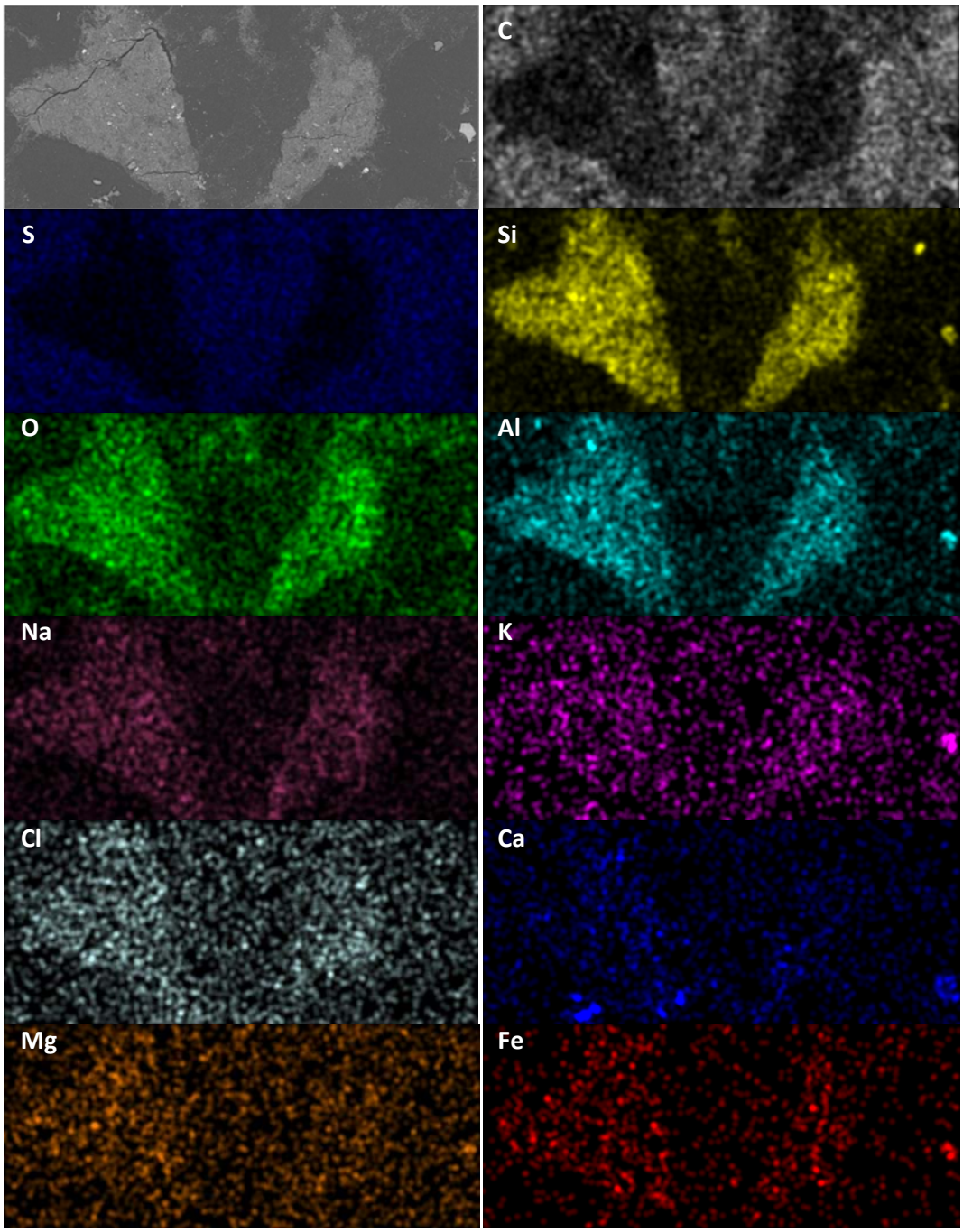

Figure 4: Elemental mapping of scale deposits on a used RO membrane surface which had treated first stage RO brine derived from CSG water

3.3.4 FTIR Analysis of Scale Deposits on Used RO Membrane

Infrared spectra were acquired for both a fresh membrane sample and one which had been used in a secondary RO unit treating CSG brine. The IR spectrum for the fresh sample was characteristic of polysulfone support layer and the polyamide active layer [45]. To facilitate

identification of vibrations due to foulant species, the spectrum for the fresh membrane was subtracted from the spectrum of a used membrane [Figure 5]. The subtraction spectrum exhibited peaks at approximately 1625, 1025, 550 and 475 cm^{-1}. Several authors have reported bands characteristic of organic foulants including proteins and polysaccharides which may arise from microorganisms or humic substances appear at 1631 cm^{-1} (C=O stretch) and 1078 cm^{-1} (C-O stretch of polysaccharide) [36, 46].

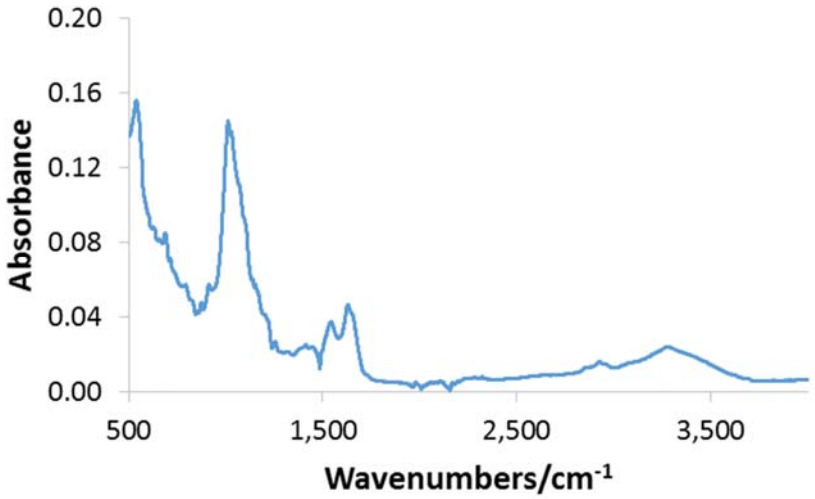

Figure 5: Difference FTIR spectrum generated by subtracting spectrum of used RO membrane from spectrum of fresh membrane

Howe *et al.* [47] reported that deposits on a membrane used for filtration of natural river and lake water displayed a major FTIR band at 1034 cm^{-1} which was ascribed to Si-O stretching vibrations. Howe *et al.* [47] also recorded bands at 3699, 3653, and 3622 cm^{-1} which were assigned to hydroxyl vibrations of aluminosilicate species. There latter peaks were absent in our study and only a broad band due to water was seen in this latter spectral region. Nevertheless, the aluminosilicate detected in this study from the SEM/EDS analysis was sodium exchanged and thus hydroxyl groups were expected not to be present. The infrared analysis cannot unequivocally differentiate between organic species on the resin surface and the presence of an aluminosilicate or silicate material.

Through membrane autopsy, aluminium silicates and silica have been identified as probably the primary species responsible for scale formation. Elemental mapping was consistent

with albite being potentially the major phase as suggested by PHREEQC calculations. However, a definitive assessment regarding the phase cannot be made. For phase determination, a technique such as XRD analysis would be required. It is noted that previous membrane autopsy studies which have successfully employed XRD have typically involved membranes from pilot facilities that have been in operation for long periods of time [46], leading to large scale deposits that were readily separated from the membrane by physical scraping or sonication. In this study, the scaled membrane had not been in operation for more than a few weeks and the scale layer was therefore not fully developed. Consequently, no scale could be separated for XRD analysis either by physical scraping or sonication. Calcium and iron based species were also identified in the autopsy as minor additional scalants. These findings agree with the scalants predicted in PHREEQC, in that aluminium silicates were a key predicted scalant, alongside calcium and iron based scalants. Silica removal will therefore be of primary interest when evaluating the performance of either coagulants or NF membranes as a potential pre-treatment step, while aluminium, iron, and calcium removal will also be considered.

3.4 Coagulant Tests to Remove Dissolved Silica

The degree of silica removal from CSG brine by application of ACH coagulant was evaluated. These experiments were designed to not only determine if coagulants could remove dissolved silica species from brine but also to provide a baseline by which to evaluate nanofiltration performance (as coagulation is usually less costly than a nanofiltration process). Table 4 shows that the extent of silica removal from the brine was related to the amount of coagulant added.

Table 4: Degree of dissolved silica removal from ACH addition to RO brine

Volume of ACH Added (µL/L)	% Si Removal
2000	70.5
1000	51.7
500	24.9
200	11.3
100	3.1

Sanciolo *et al.* [39] and Salvador Cob *et al*. [48] showed that dissolved silicate was removed from solution by aluminium hydroxide ($Al(OH)_3$) species at alkaline pH values. Milne *et al.* [27] outlined that the essential feature was M-OH groups which bound dissolved silica species. Here the formation of aluminium hydroxide species when ACH was added as a coagulant to the CSG brine occurred and thus facilitated removal of problematic silica moieties.

3.5 ROSA Analysis of Predicted Membrane Performance

ROSA software is widely used to aid in the prediction of membrane performance for applications such as desalination [23, 24, 49, 50]. Figure 6 presents the results of ROSA simulation of two membranes (NF90 and NF270) with regards to treatment of RO brine.

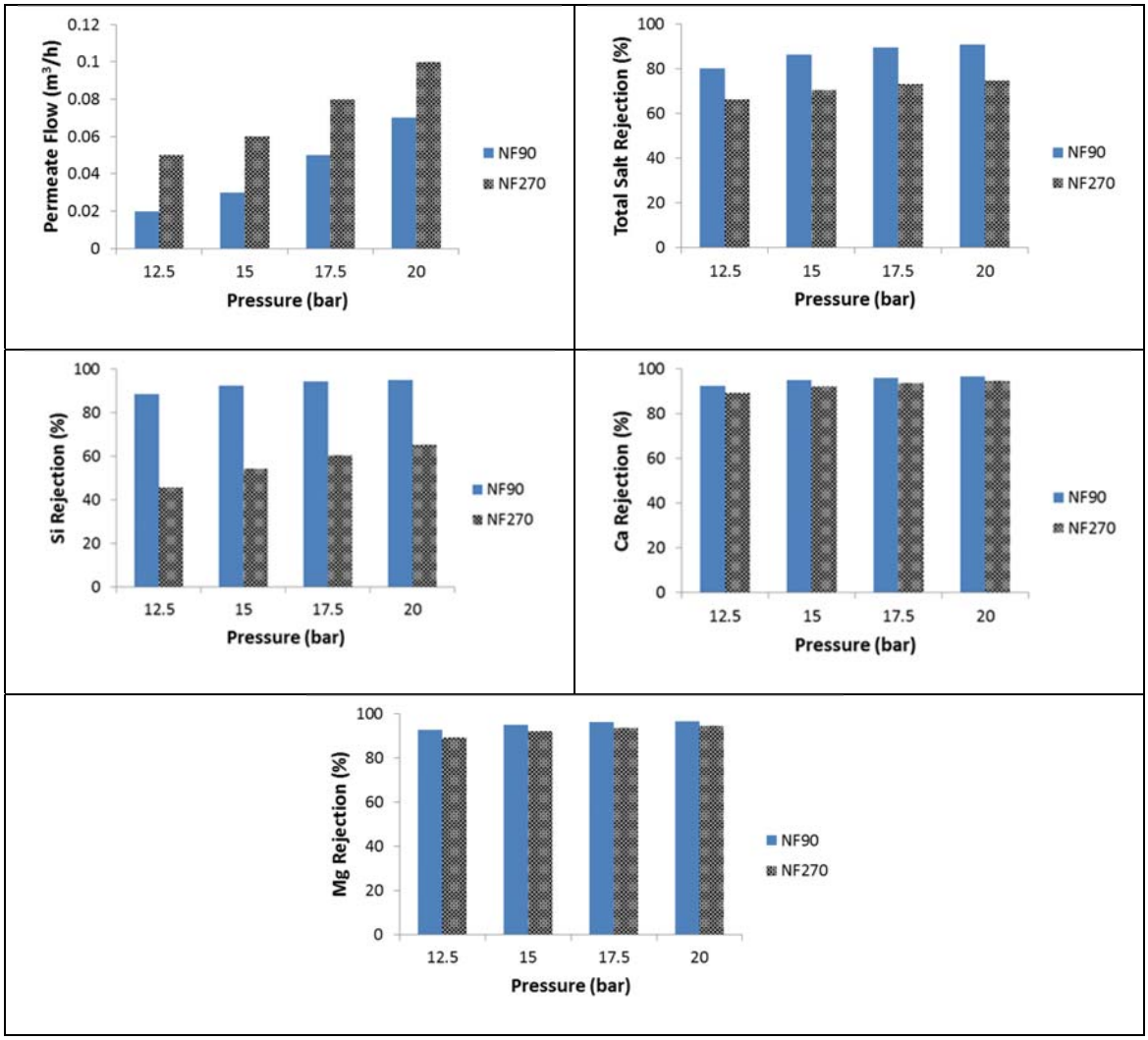

Figure 6: ROSA predictions for NF membrane performance when treating RO brine

In general, the looser [40] NF270 membrane was able to achieve higher permeate flux and recovery values than the NF90 membrane at the same operating pressure, while the latter offered greater rejection values. Calcium and magnesium rejection values were similar for the two membranes, therefore NF270 should in theory be sufficient in the context of hardness based scale prevention. Silica based scale prevention was the principal concern in this case, and NF90 offered considerably higher silica rejection values than NF270. For example, at 20 bar pressure, the predicted silica rejection of NF90 was 95.06 %, while that of NF270 was 65.09 %. Consequently, based on these latter predictions it appeared that NF90 membrane may be preferred over NF270 for pre-treatment of the CSG brine. According to ROSA, the osmotic pressure of the CSG brine was approximately 12.7 bar. For both membranes, permeate flux, recovery and rejection values increased as the operating pressure increased above this latter value, however, the energy requirements of the system also increased. For NF90, the predicted silica rejection increased by just 0.83 % between 20 and 25 bar, while for NF270 it did not increase at all, indicating that above 20 bar the minimal increase in performance may not justify the increased energy demand.

3.6 Nanofiltration of CSG brine

Four membranes were chosen with respect to practical testing of NF performance using coal seam brine solution [Figure 7].

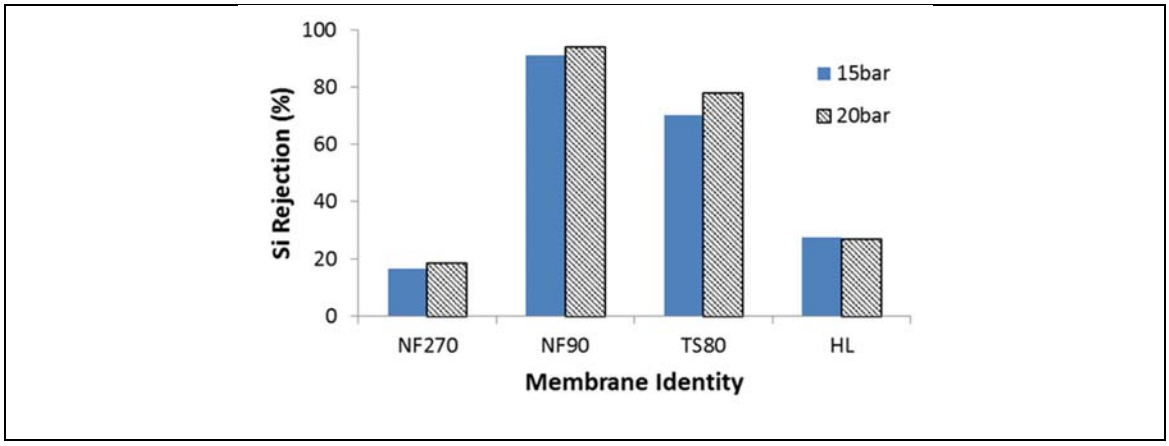

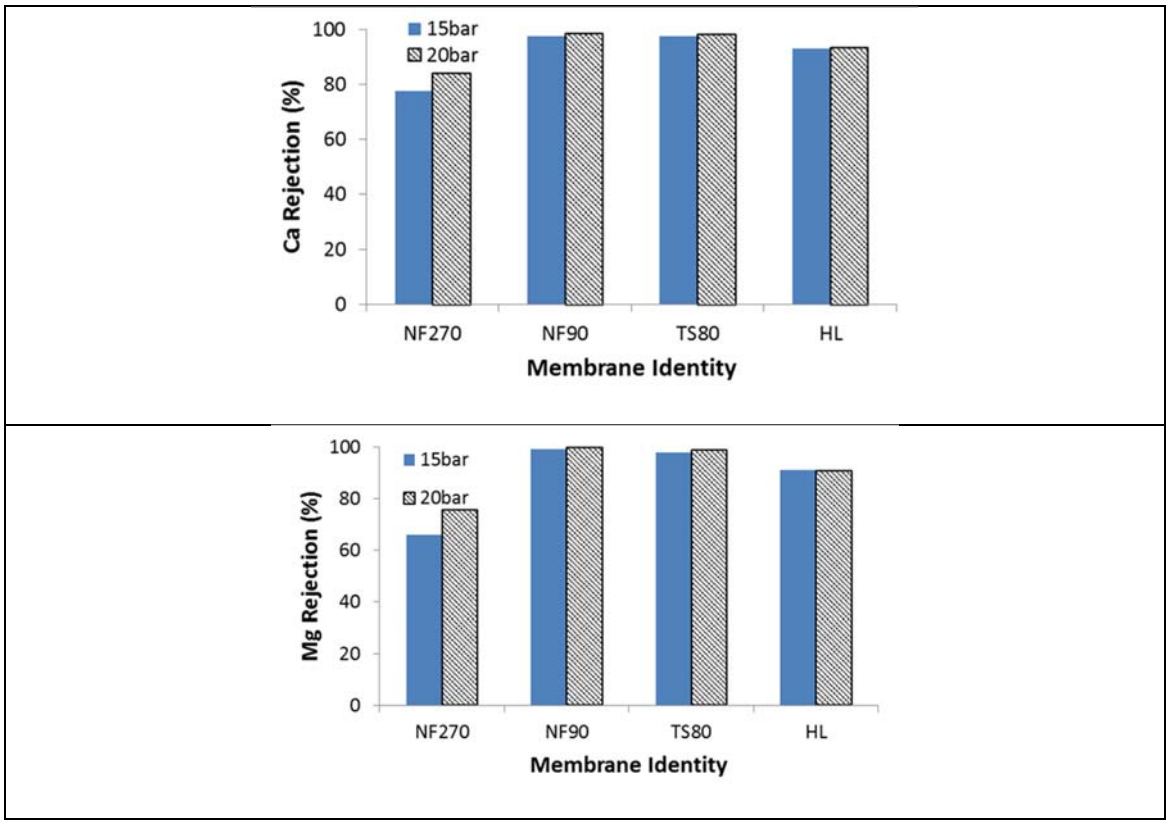

Figure 7: Performance of a variety of NF membranes for treatment of CSG brine

In terms of silica rejection, there was a definite relationship between permeate flux values and silicon rejection, in that the membranes with lower flux exhibited higher rejection. This was expected given that lower flux values correspond to "tighter" membranes [40], which restrict convective transport and therefore have better rejection performance. Notably, the actual performance of NF270 membrane was significantly less than predicted by ROSA software (*e.g.* 18.5 instead of 45.6 % rejection at 20 bar pressure, respectively). In contrast, there was excellent agreement between the theoretical and experimental silica rejection values for NF90 membrane (*e.g.* 95.1 and 94 % rejection at 20 bar pressure, respectively). The latter data was consistent with evidence presented by Xu *et al.* which suggested that 96 % rejection of silica could be achieved by NF90 membrane when used to treat CSG water from Montana [45].

The performance of NF270 membrane was similarly less than predicted in terms of calcium ion rejection (e.g. 84.1 instead of 94.9 % rejection at 20 bar pressure, respectively).

Whereas, NF90 membrane performed in accord with calculations (e.g. 98.5 and 96.7 % rejection at 20 bar pressure, respectively). Again the testing data was in harmony with nanofiltration softening of CSG water by Xu *et al.* wherein 98 % calcium rejection at lab-scale with a DOW Filmtec NF90 membrane operated at 12.5 bar was noted [45]. A similar situation to calcium ions was recorded for the magnesium removal data using NF membranes in this study.

Based upon the simulated and actual experimental data, the recommended membrane to use for nanofiltration prior to the second stage RO unit is NF90. As for operating pressure, the permeate flow for NF90 increased substantially from 0.03 to 0.07 m^3/h upon raising the pressure from 15 to 20 bar, thus 20 bar appears preferable (but detailed economic calculations required to confirm). The key limiting factor in NF softening is that in the course of rejecting scalant species, the NF membranes can themselves be susceptible to scale formation [51].

Future work should focus on operating the NF membranes for longer timeframes to determine if they exhibit decreasing flux rates and what cleaning in place procedures are required to regenerate performance. Fouling of nanofiltration membranes is known by a range of species such as organic materials [52, 53]. Hence, it is important to determine the level of fouling and whether nanofiltration membrane incorporation as an intermediate filtration stage in a dual RO system is viable. The issue of what to do with the produced brine from the NF is one which also needs to be addressed. One option is to simply add to the RO brine pond which is usually on site, or to explore salt recovery strategies. In addition, the performance of the ACH coagulant was prospective and studies should be expanded to determine if ACH is the optimal coagulant to use and in addition if a coagulation process prior to the NF stage is beneficial.

4. Conclusions

Application of a dual stage reverse osmosis unit for concentration of coal seam brine produced from a coal seam gas operation, was found to suffer from fouling of the membrane surface. Theoretical calculations in relation to saturation index indicated that a range of materials could potentially deposit on the membrane surface. Application of SEM

and EDS detected aluminosilicate formation in addition to silica. The degree of fouling was relatively light due to relatively brief testing periods for the membrane.

Simple coagulation of brine from a first stage RO unit using aluminium chlorohydrate was surprisingly effective with regards to reducing the concentration of dissolved silica species from CSG brine (up to 70.5 %). Coagulation of the brine may prove attractive in terms of protecting downstream membranes used to further concentrate the brine.

Nanofiltration prior to the secondary RO stage was found to be beneficial in terms of removal of silica, calcium, and magnesium species. Tight NF90 membrane was superior in terms of ion rejection compared to the looser NF270 membrane, but did exhibit reduced permeate flow relative to NF270. An operating pressure of 20 bar was recommended as it significantly increased the flux rate when using NF90 membrane.

Future work should focus on determining the long term stability of the nanofiltration membrane during brine concentration. Further work should be directed towards the employment of other softening methods such as coagulation or indeed ion exchange to discover if nanofiltration is either competitive to the aforementioned techniques or can be enhanced in performance by use in combination with alternate technologies.

5. Acknowledgements

We would like to thank the coal seam gas operator who supplied the brine sample from their operating reverse osmosis facility for treating CSG water. We also thank the membrane supplier who donated used reverse osmosis membrane from their brine concentration system.

6. References

[1] G.J. Millar, S.J. Couperthwaite, C.D. Moodliar, Strategies for the management and treatment of coal seam gas associated water, Renewable and Sustainable Energy Reviews, 57 (2016) 669-691.
[2] T.A. Moore, Coalbed methane: A review, International Journal of Coal Geology, 101 (2012) 36-81.
[3] I. Hamawand, T. Yusaf, S.G. Hamawand, Coal seam gas and associated water: A review paper, Renewable and Sustainable Energy Reviews, 22 (2013) 550-560.
[4] S. Khan, G. Kordek, Coal seam gas: Produced water and solids, in, 2014.
[5] M.H. Plumlee, J.F. Debroux, D. Taffler, J.W. Graydon, X. Mayer, K.G. Dahm, N.T. Hancock, K.L. Guerra, P. Xu, J.E. Drewes, T.Y. Cath, Coalbed methane produced water screening tool for treatment technology and beneficial use, Journal of Unconventional Oil and Gas Resources, 5 (2014) 22-34.
[6] L.D. Nghiem, T. Ren, N. Aziz, I. Porter, G. Regmi, Treatment of coal seam gas produced water for beneficial use in australia: A review of best practices, Desalination and Water Treatment, 32 (2011) 316-323.
[7] R. Dennis, Ion exchange helps CBM producers handle water, Oil and Gas Journal, 105 (2007) 41-43.
[8] Z. Qian, X. Liu, Z. Yu, H. Zhang, Y. JÜ, A Pilot-scale Demonstration of Reverse Osmosis Unit for Treatment of Coal-bed Methane Co-produced Water and Its Modeling, Chinese Journal of Chemical Engineering, 20 (2012) 302-311.
[9] A. Simon, T. Fujioka, W.E. Price, L.D. Nghiem, Sodium hydroxide production from sodium carbonate and bicarbonate solutions using membrane electrolysis: A feasibility study, Separation and Purification Technology, 127 (2014) 70-76.
[10] H.C. Duong, M. Duke, S. Gray, B. Nelemans, L.D. Nghiem, Membrane distillation and membrane electrolysis of coal seam gas reverse osmosis brine for clean water extraction and NaOH production, Desalination, 397 (2016) 108-115.
[11] J. Morillo, J. Usero, D. Rosado, H. El Bakouri, A. Riaza, F.-J. Bernaola, Comparative study of brine management technologies for desalination plants, Desalination, 336 (2014) 32-49.
[12] A. Antony, J.H. Low, S. Gray, A.E. Childress, P. Le-Clech, G. Leslie, Scale formation and control in high pressure membrane water treatment systems: A review, Journal of Membrane Science, 383 (2011) 1-16.
[13] S.R. Pandey, V. Jegatheesan, K. Baskaran, L. Shu, Fouling in reverse osmosis (RO) membrane in water recovery from secondary effluent: A review, Reviews in Environmental Science and Biotechnology, 11 (2012) 125-145.
[14] S. Salvador Cob, C. Beaupin, B. Hofs, M.M. Nederlof, D.J.H. Harmsen, E.R. Cornelissen, A. Zwijnenburg, F.E. Genceli Güner, G.J. Witkamp, Silica and silicate precipitation as limiting factors in high-recovery reverse osmosis operations, Journal of Membrane Science, 423-424 (2012) 1-10.
[15] J. Welch, Reverse osmosis treatment of CBM produced water continues to evolve, Oil and Gas Journal, 107 (2009) 45-50.
[16] K.P. Lee, T.C. Arnot, D. Mattia, A review of reverse osmosis membrane materials for desalination-Development to date and future potential, Journal of Membrane Science, 370 (2011) 1-22.
[17] J. Gilron, Brine Treatment and High Recovery Desalination, in: Emerging Membrane Technology for Sustainable Water Treatment, 2016, pp. 297-324.
[18] R. Günther, B. Perschall, D. Reese, J. Hapke, Engineering for high pressure reverse osmosis, Journal of Membrane Science, 121 (1996) 95-107.
[19] Y. Liu, X. Li, B. Wang, S. Liu, Performance of landfill leachate treatment system with disc-tube reverse osmosis units, Frontiers of Environmental Science and Engineering in China, 2 (2008) 24-31.
[20] N. Hilal, H. Al-Zoubi, N.A. Darwish, A.W. Mohammad, M. Abu Arabi, A comprehensive review of nanofiltration membranes: Treatment, pretreatment, modelling, and atomic force microscopy, Desalination, 170 (2004) 281-308.

[21] N. Hilal, H. Al-Zoubi, N.A. Darwish, A.W. Mohammad, Performance of nanofiltration membranes in the treatment of synthetic and real seawater, Separation Science and Technology, 42 (2007) 493-515.
[22] R. Rautenbach, T. Linn, L. Eilers, Treatment of severely contaminated waste water by a combination of RO, high-pressure RO and NF - Potential and limits of the process, Journal of Membrane Science, 174 (2000) 231-241.
[23] M. Azadi Aghdam, F. Zraick, J. Simon, J. Farrell, S.A. Snyder, A novel brine precipitation process for higher water recovery, Desalination, 385 (2016) 69-74.
[24] Y. Aroussy, M. Nachtane, D. Saifaoui, M. Tarfaoui, M. Rouway, Thermodynamic performance evaluation of a reverse osmosis and nanofiltration desalination, International Journal of Applied Engineering Research, 11 (2016) 9149-9153.
[25] G.J. Millar, J. Lin, A. Arshad, S.J. Couperthwaite, Evaluation of electrocoagulation for the pre-treatment of coal seam water, Journal of Water Process Engineering, 4 (2014) 166-178.
[26] W.S. Walker, Y. Kim, D.F. Lawler, Treatment of model inland brackish groundwater reverse osmosis concentrate with electrodialysis ? Part II: Sensitivity to voltage application and membranes, Desalination, 345 (2014) 128-135.
[27] N.A. Milne, T. O'Reilly, P. Sanciolo, E. Ostarcevic, M. Beighton, K. Taylor, M. Mullett, A.J. Tarquin, S.R. Gray, Chemistry of silica scale mitigation for RO desalination with particular reference to remote operations, Water Research, 65 (2014) 107-133.
[28] K.G. Dahm, K.L. Guerra, P. Xu, J.E. Drewes, Composite geochemical database for coalbed methane produced water quality in the Rocky Mountain region, Environmental Science and Technology, 45 (2011) 7655-7663.
[29] C.A. Rice, Production waters associated with the Ferron coalbed methane fields, central Utah: chemical and isotopic composition and volumes, International Journal of Coal Geology, 56 (2003) 141-169.
[30] X. Li, B. Gao, Q. Yue, D. Ma, H. Rong, P. Zhao, P. Teng, Effect of six kinds of scale inhibitors on calcium carbonate precipitation in high salinity wastewater at high temperatures, Journal of Environmental Sciences, 29 (2015) 124-130.
[31] B. Van der Bruggen, M. Mänttäri, M. Nyström, Drawbacks of applying nanofiltration and how to avoid them: A review, Separation and Purification Technology, 63 (2008) 251-263.
[32] W. Hater, C. zum Kolk, G. Braun, J. Jaworski, The performance of anti-scalants on silica-scaling in reverse osmosis plants, Desalination and Water Treatment, 51 (2013) 908-914.
[33] A. Sweity, Y. Oren, Z. Ronen, M. Herzberg, The influence of antiscalants on biofouling of RO membranes in seawater desalination, Water Research, 47 (2013) 3389-3398.
[34] T. Tran, B. Bolto, S. Gray, M. Hoang, E. Ostarcevic, An autopsy study of a fouled reverse osmosis membrane element used in a brackish water treatment plant, Water Research, 41 (2007) 3915-3923.
[35] C.J. Gabelich, M.D. Williams, A. Rahardianto, J.C. Franklin, Y. Cohen, High-recovery reverse osmosis desalination using intermediate chemical demineralization, Journal of Membrane Science, 301 (2007) 131-141.
[36] N. Melián-Martel, J.J. Sadhwani, S. Malamis, M. Ochsenkühn-Petropoulou, Structural and chemical characterization of long-term reverse osmosis membrane fouling in a full scale desalination plant, Desalination, 305 (2012) 44-53.
[37] M. Uchymiak, A. Rahardianto, E. Lyster, J. Glater, Y. Cohen, A novel RO ex situ scale observation detector (EXSOD) for mineral scale characterization and early detection, Journal of Membrane Science, 291 (2007) 86-95.
[38] M. Zaman, G. Birkett, C. Pratt, B. Stuart, S. Pratt, Downstream processing of reverse osmosis brine: Characterisation of potential scaling compounds, Water Research, 80 (2015) 227-234.
[39] P. Sanciolo, N. Milne, K. Taylor, M. Mullet, S. Gray, Silica scale mitigation for high recovery reverse osmosis of groundwater for a mining process, Desalination, 340 (2014) 49-58.

[40] A. Subramani, R. Schlicher, J. Long, J. Yu, S. Lehman, J.G. Jacangelo, Recovery optimization of membrane processes for treatment of produced water with high silica content, Desalination and Water Treatment, 36 (2011) 297-309.
[41] I. Bibi, J. Icenhower, N.K. Niazi, T. Naz, M. Shahid, S. Bashir, Clay Minerals: Structure, Chemistry, and Significance in Contaminated Environments and Geological CO2 Sequestration, in: Environmental Materials and Waste: Resource Recovery and Pollution Prevention, 2016, pp. 543-567.
[42] S.P. Chesters, Innovations in the inhibition and cleaning of reverse osmosis membrane scaling and fouling, Desalination, 238 (2009) 22-29.
[43] B. Tomaszewska, M. Bodzek, Desalination of geothermal waters using a hybrid UF-RO process. Part II: Membrane scaling after pilot-scale tests, Desalination, 319 (2013) 107-114.
[44] L. Lunevich, P. Sanciolo, A. Smallridge, S.R. Gray, Silica scale formation and effect of sodium and aluminium ions -29Si NMR study, Environmental Science: Water Research and Technology, 2 (2016) 174-185.
[45] P. Xu, J.E. Drewes, D. Heil, Beneficial use of co-produced water through membrane treatment: technical-economic assessment, Desalination, 225 (2008) 139-155.
[46] I.M. El-Azizi, R.G.J. Edyvean, Performance evaluation and fouling characterisation of two commercial SWRO membranes, Desalination and Water Treatment, 5 (2009) 34-41.
[47] K.J. Howe, K.P. Ishida, M.M. Clark, Use of ATR/FTIR spectrometry to study fouling of microfiltration membranes by natural waters, Desalination, 147 (2002) 251-255.
[48] S. Salvador Cob, B. Hofs, C. Maffezzoni, J. Adamus, W.G. Siegers, E.R. Cornelissen, F.E. Genceli Güner, G.J. Witkamp, Silica removal to prevent silica scaling in reverse osmosis membranes, Desalination, 344 (2014) 137-143.
[49] S.Y. Alnouri, P. Linke, Optimal Membrane Desalination Network Synthesis with Detailed Water Quality Information, in: Computer Aided Chemical Engineering, 2012, pp. 520-524.
[50] S.Y. Alnouri, P. Linke, Optimal design of SWRO desalination processes with boron level considerations, in: Computer Aided Chemical Engineering, 2013, pp. 799-804.
[51] L.F. Greenlee, D.F. Lawler, B.D. Freeman, B. Marrot, P. Moulin, Reverse osmosis desalination: Water sources, technology, and today's challenges, Water Research, 43 (2009) 2317-2348.
[52] F. Gao, Y. Sheng, H. Cao, Y. Li, C. Su, X. Cui, The synergistic effect of organic foulants and their fouling behavior on the nanofiltration separation to multivalent ions, Desalination and Water Treatment, 57 (2016) 29044-29057.
[53] M. Park, T. Anumol, J. Simon, F. Zraick, S.A. Snyder, Pre-ozonation for high recovery of nanofiltration (NF) membrane system: Membrane fouling reduction and trace organic compound attenuation, Journal of Membrane Science, 523 (2017) 255-263.